

First-principles Study of Structure, Energetic and Infrared Spectrum for Ice Ih

N.Tsogbadrakh* and Sh. Dashpurev

Department of Theoretical and Experimental Physics, School of Physics and Electronics,
National University of Mongolia, University Street 1, Ulaanbaatar-210646, Mongolia
*E-mail: Tsogbadrakh@num.edu.mn

We present the results of density functional based computational study of structure, cohesive energy and IR spectrum of ice Ih, and compared with the experimental results. Within the our computational framework the sensitive to calculated structural properties including the zero point vibrations is estimated and shown to be small even though changes in zero point energies account for a significant fraction of the cohesive energy.

Keywords: ice, zero point energy (ZPE), cohesive energy, *ab-initio* IR spectrum

I. INTRODUCTION

The simulation of infrared (IR) spectrums of condensed materials by theoretical methods is not an easy task. The first-principles (*ab-initio*) IR spectrum has been carried out along either of the following schemes. The first simulation scheme is performed within the harmonic approximation at low temperatures. It requires the calculation of the vibrational frequencies by diagonalization of the dynamical matrix and the Born (transverse) effective charge tensor. These two quantities are the second derivatives of the energy, and can be obtained by a finite difference method. The application of this scheme usually involves several stages to be performed with an acceptable numerical precision. The first stage is to relax the structure to its theoretical equilibrium configuration. The next stage is the evaluation of the force constants, which is calculated from the variations in the atomic forces, which arise for small displacements of the atoms around their equilibrium configuration. This process is very time consuming, and the calculation of the vibrational frequencies is fairly straightforward, being given by the eigenvalues of the dynamical matrices. The corresponding eigenvectors provide a representation of the motions of each atom per vibrational modes. The second simulation scheme is the Car-Parrinello molecular dynamic (CPMD) simulation at high temperatures, and the macroscopic polarization of solids is evaluated at each step of a trajectory, and then the dipole-dipole correlation function, which is directly related to the IR absorbance, is evaluated. This scheme is especially suitable when dealing with liquids or anharmonic systems.

We present the results of density functional based computational study of structure, cohesive energy and *ab initio* IR spectrum on the example of ice Ih, and compared with the experimental results,

which are measured at the Central Laboratory of Natural Science (CLNS) in the Mongolian Academy of Science (MAS). Ice is a weakly hydrogen bonded molecular solid. A hydrogen bond is a type of attractive intermolecular force that exists between two partial electric charges of opposite polarity. Ice is a model material, and provides understanding applicable to many hydrogen bonded molecular solids.

This paper is constructed as follows. In Sec. II we briefly describe the theory of the *ab initio* IR spectrum, and in Sec. III we describe the computational methods used in our study. In Sec. IV we present the results and discussions of density functional based structure, cohesive energy and IR spectrum for tetrahedrally fully coordinated ice Ih, and compare with experimental values. Finally we set out our conclusions in Sec. V.

II. THEORY

We can address the calculation of the IR absorption of the crystal. For a molecule in the gas phase, the IR absorbance of m^{th} normal mode is given by[1]

$$I_{IR}^m = \frac{\rho\pi}{3c} \left| \frac{\partial \vec{\mu}}{\partial Q_m} \right|^2 \quad (1)$$

where ρ is the molecular concentration, c is the velocity of light and $\vec{\mu}$ is the electric dipole moment, and Q_m is the normal mode coordinate

$$U_{j,m}^\tau = Q_m X_{j,m}^\tau \quad (2)$$

Here $U_{j,m}^\tau$ is the m^{th} normal mode component of the displacement of the atom τ in the direction, evaluated from the $X_{j,m}^\tau$ elements of the corresponding vibrational eigenvectors.

A similar expression can be used for solid polycrystalline samples, replacing the electric dipole moment by the macroscopic polarization[2]

$$I_{IR}^m \propto \sum_{i=1}^3 \left(\frac{\partial P_i}{\partial Q_m} \right)^2 \quad (3)$$

where P_i is the i component of the macroscopic polarization and eigenmodes are calculated at the Γ point. The Eq. (3) is valid for solids under two main approximations. First, we suppose that the material is a polycrystal where all directions are equivalent. This is the same as saying that the angle between the crystalline axis and the electric field of the incident IR light is random. Second, we ignore the effects of macroscopic shape of the sample, which are mainly transmission-reflection and interference effects. These could be taken into account by constructing a macroscopic electromagnetic model suitable for each specific problem. The derivative in Eq. (3) can be rewriting in terms of the Born (transverse) effective charge tensor so that the IR absorbance for the m^{th} mode results

$$I_{IR}^m \propto \sum_{i=1}^3 \left(\sum_{j=1}^3 \sum_{\tau=1}^N Z_{ij,\tau}^* X_{j,m}^\tau \right)^2 \quad (4)$$

where N is the number of atoms in the unit cell, and $Z_{ij,\tau}^*$ is the Born (transverse) effective charge tensor, which is defined as the linear change in the polarization per unit cell created along the direction i when the atom τ is displaced along the direction j

$$Z_{ij,\tau}^* = V \frac{\partial P_i}{\partial r_j^\tau} \quad (5)$$

where V is the volume of the unit cell, r_j^τ is the displacement of the atom τ along the j axis. Here the direct evaluation of $\Delta \vec{P}$ is cumbersome in numerical calculations, because in practice we only compute the wave functions at a finite number of points in the Brillouin Zone (BZ), and in general there will be no particular phase relationship between the eigenvectors generated by the diagonalization routine. In actual calculations we circumvent this difficulty using the following strategy. First, we pick a direction parallel to a short reciprocal lattice vector of the solid, \vec{G}_\parallel . Second, we choose the primitive cell for the \vec{k} -space integration to be prism with its axis aligned along

\vec{G}_\parallel . The component of $\Delta \vec{P}$ directed along \vec{G}_\parallel can be written as[3]:

$$\Delta P_\parallel = P_\parallel^{(1)} - P_\parallel^{(0)} \quad (6)$$

where, in a notation

$$\vec{P}_\parallel = \frac{ifq_e}{8\pi^3} \int_S d\vec{k}_\perp \sum_{n=1}^M \int_0^{|\vec{G}_\parallel|} d\vec{k}_\parallel \left\langle u_{kn}^{(\lambda)} \left| \frac{\partial}{\partial k_\parallel} \right| u_{kn}^{(\lambda)} \right\rangle \quad (7)$$

where q_e is the electron charge, f is the occupation number of states in the valence band (in spin degenerate systems $f=2$), M is the number of occupied bands and $u_{kn}^{(\lambda)}$ is the periodic wave function. The integration in the perpendicular direction is easy and can be performed by sampling over a 2D mesh of \vec{k} -points generated. To perform the integral over \vec{k}_\parallel at each point in the \vec{k}_\perp mesh, we compute the cell periodic parts of wave functions at the string of J \vec{k} -points at $\vec{k}_j = \vec{k}_\perp + j\vec{G}_\parallel/J$ where j runs from 0 to $J-1$.

At the high temperature, the IR absorption is proportional to the imaginary part of the dielectric function in the classic limit from the following formula[4]:

$$\text{Im } \varepsilon(\omega) = \frac{2\pi\omega}{3Vk_B T} \int_{-\infty}^{+\infty} dt e^{-i\omega t} \langle \vec{\mu}(t) \cdot \vec{\mu}(0) \rangle \quad (8)$$

where $\vec{\mu}$ is the total dipole moment and the angular brackets indicate the statistical average.

The correlation function $\langle \vec{\mu}(t) \cdot \vec{\mu}(0) \rangle$ is the computed directly in the CPMD simulation. The electronic contribution to $\vec{\mu}$ is computed by using Berry phase approximation.

III. COMPUTATIONAL METHODS

The calculations of structure optimizations and vibrational frequencies were performed within the framework of density functional based tight binding approximation (TBA) using the LCAO method, as employed in the SIESTA code[5,6]. When liquid water freezes, the hexagonal structure (iceIh) for oxygen atoms with proton disordered arrangements generates in the condensed phase. The hydrogen atoms are located by the Bernal-Fowler ice rules[7]. The space group for the average structure with a half hydrogen on each possible site is $P6_3/mmc$, and the (c/a) ratio of the hexagonal lattice parameters is

almost independent of temperature at 1.62806 ± 0.00009 for H_2O ice[8]. The most precise measurements of the lattice parameters were made by K. Rottger *et al.*[9] using synchrotron radiation, and were subsequently confirmed by Line and Whitworth[10] using neutrons. The supercell chosen for our calculations consists of 16 water molecules in an orthorhombic unit cell[11]. This is relatively small unit cell, but compatible with computational constraints imposed by the *ab initio* simulation. The valence electrons of atoms in ice are described by the self-consistent solution to the Kohn-Sham equations with the PBE-GGA exchange correlation functional. In order to integrate over the BZ, we used 8K points as the Monkhorst-Pack scheme[12]. Periodic boundary conditions are employed. The interactions of valence electrons with the atomic ionic cores are described by the norm conserving pseudopotentials with the partial core correction of $0.6a.u.$ on the oxygen atom[13]. We used the various *double zeta plus polarization (DZP)* basis sets. A mesh cut-off energy $350Ry$, which defines the equivalent plane wave cut-off for the grid, was used. The forces on atomic ions are obtained by the Hellman-Feynman theorem and were used to relax atomic ionic positions to the minimum energy. The atomic forces within the supercell were minimized to within $0.005eV/\text{\AA}$. In order to find vibrational frequencies and IR absorbance, we used a finite different method from the calculation of the *ab initio* total energy and forces, and found a zone centre force constant matrix using the VIBRA program. Here the shift is chosen to be 0.02\AA . When we compute the macroscopic polarization using the Eq.(7), we used the polarization grid of $(10 \times 7 \times 7)$ in the \vec{k} -space. After found the vibrational frequencies and eigenvectors, we have used the Eq.(4), in order to found the IR intensities on the each vibration modes. In order to facilitate presentation, each mode has been broadened by the Lorentzian function of half width of 100cm^{-1} at the half maximum[14]. This value is chosen as optimal in retaining the essential features of the IR absorbance.

IV. RESULTS AND DISCUSSIONS

A. The Structure of iceIh

At the zero temperature, the condition for the stable structure at constant pressure is that enthalpy be minimum. In order to find the equilibrium configuration with the various DZP basis sets, the supercells were relaxed as both the atomic ionic positions and lattice parameters. The structure optimization calculations were done by varying the volume of the supercells, and the minimum energy was evaluated. Since the calculations were performed at the zero temperature and pressure, we compare them with data at the lowest available temperature extrapolated to atmospheric pressure [15]. We have shown the calculated total energy curves for iceIh on Fig.1. In our calculation the relaxed lattice parameters were found to be 3.50% smaller than the experimental lattice parameters as both the delocalized DZP basis set and the optimized - DZP basis set with long localization. In the choice of the medium optimized - DZP basis set with the medium localization, the relaxed lattice parameters were found to be 1.75% smaller than the experimental lattice parameters. In the localized - DZP basis set solved by the order-N method[5], the relaxed lattice parameters were found to be 3.0% smaller than the experimental lattice parameters. The lattice parameters of a crystal can never actually have the correct energy, because it must always have some vibrational motions of atoms or molecules in a solid. We have presented the above results and their lattice energies on Table 1. It is shown that the relaxed lattice parameters depend on the choice of the basis sets, and the best numerical atomic basis set in our supercells is the optimized - DZP basis set with the medium localizations.

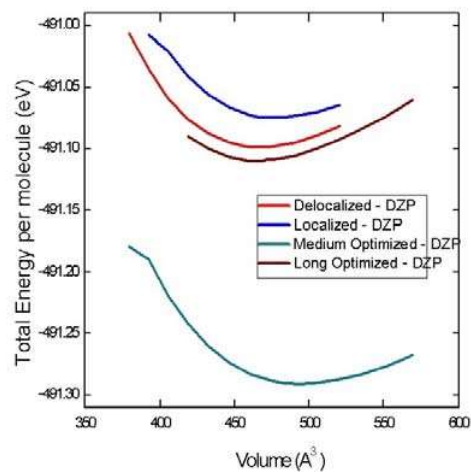


Fig.1. The total energy curves of the structure for iceIh[13]

Table 1. The calculated lattice energies and lattice parameters of the relaxed primitive hexagonal unit cell for iceIh [13].

	experimental values	Delocalized - DZP	Localized- DZP	Optimized-DZP	
				Medium	Long
c (\AA)	7.357	7.0995	7.1363	7.2283	7.0995
a (\AA)	4.519	4.3608	4.3834	4.4399	4.3608
Error (%)		<3.50	<3.00	<1.75	<3.50
E_{lattice} (eV / molecule)		-491.0990	-491.0746	-491.2912	-491.1102

Table 2. The calculated lattice energies and lattice parameters of the relaxed primitive hexagonal unit cell for iceIh including the ZPE [13].

	experimental values	Delocalized - DZP	Localized- DZP	Optimized-DZP	
				Medium	Long
c (\AA)	7.357	7.0995	7.1731	7.2283	7.0995
a (\AA)	4.519	4.3608	4.4060	4.4399	4.3608
Error (%)		<3.50	<2.50	<1.75	<3.50
$E_{\text{lattice}} + E_{\text{lattice}}^{\text{ZPE}}$ (eV / molecule)		-490.4037	-490.3662	-490.5813	-490.4175

In the optimized - DZP basis set with the medium localization, the average oxygen - oxygen separation distance in ice Ih was found to be 2.73\AA , and it is 1.27% smaller than the experimentally measured value. The average O - O - O angle of a tetrahedral structure is conformed to be $109.42^\circ - 109.47^\circ$ in the various basis sets (See Fig.2). The average length of O - H covalent bonds for water molecules in iceIh is shown to be 1.00\AA . The average H - O - H angle for water molecules in iceIh was found to be 105.37° . These values were in excellent agreement with the experimental value.

B. Contributions of Zero Point Effect

The total energy computed by the structure optimization is the minimum on the total energy curve at the relaxed structure. However, the lattice parameters of a crystal can never actually have this energy because it must always have some vibrational motions of atoms or molecules in a solid. Therefore, in accurate studies, the contribution of zero point effect (ZPE) will be added to the total energy for the relaxed structure. This corrected value can then be used for computing the relative energies of various molecules and solids, and should be slightly closer to the experimental results. In our calculation there exist 144 normal vibrational frequencies corresponding to the number of degrees of freedom in the supercells with 16 water molecules. As

computed all the vibrational frequencies at the experimental and relaxed lattice parameters with the relaxed internal coordinates on the , the zero point energy could be found at the lattice parameters for ice Ih. In order to find the zero point energy on each lattice parameter, we used the linear extrapolation method. As calculated the zero point energy on each point of the lattice parameters, we have generated new total energy curves for ice Ih including the ZPE. The newly obtained total energy curves are like the curves on Fig 1. From these total energy curves we have found new minima, and presented these newly obtained lattice parameters and lattice energy on Table 2.

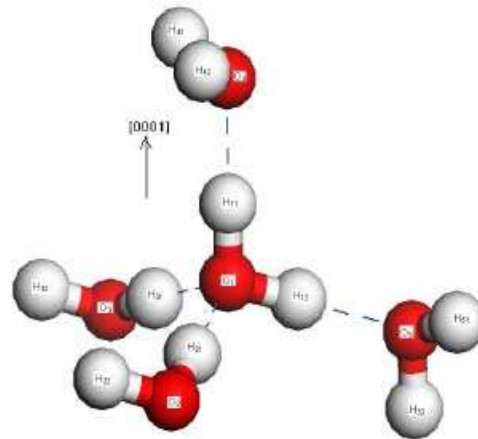


Fig.2. The tetrahedral arrangement of iceIh

C. Vibrational modes of water molecule

An individual H₂O molecule has the three normal modes of vibration illustrated in Fig. 3. The comparatively small motions of the oxygen atoms are required to keep the centre of mass stationary, and these motions result in the frequency ν_3 being slightly higher than ν_1 . These two modes depend on the force constant for stretching the covalent O - H bond, while the bending mode ν_2 depends on the force constant for changing the bond angle. In the vapour the individual molecules have a rich rotation-vibration IR spectrum[16], from which the frequencies of the molecular modes are deduced.

We also found the three normal modes of the vibration for an individual H₂O water molecule using various basis sets: symmetric stretching ν_1 , anti - symmetric stretching ν_3 and bending ν_2 for an individual water molecule. These values are chosen as optimal in retaining the essential features of the frequency spectra. Because of the limited size of

the supercell this represents an extremely coarse sampling of reciprocal space. When we calculate an individual water molecule, we have modeled the individual water H₂O molecule to be within a large cubic box with the side of 10 \AA . In the calculation of a water molecule, the XC functional and the parameters of the atomic basis set were chosen the same as for the ice, and the maximum force tolerance achieved was 0.04 eV / \AA .

We have presented the calculated total and zero point energies and vibrational modes of an individual H₂O water molecule on Table 3. It is shown that the total energy of an individual water molecule is higher than the total energy per molecule of lattice in normal ice. The zero point energy of an individual water molecule is shown to be between 554 meV and 579 meV for the various basis sets.

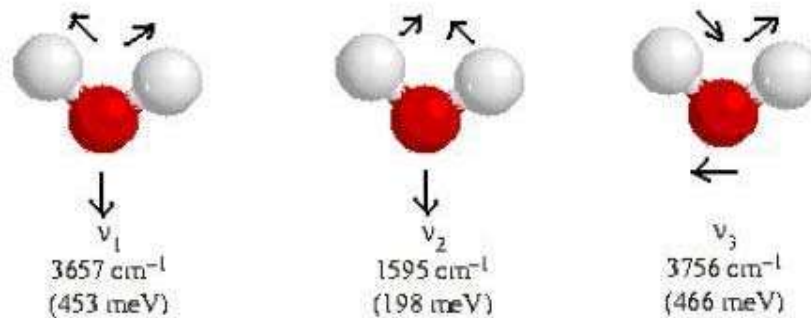


Fig.3. The three vibrational modes of an individual water H₂O molecule

Table 3. The calculated total energies and vibrational modes of an individual water H₂O molecule

	Delocalized - DZP	Localized - DZP	Optimized-DZP	
			Medium	Long
$\nu_1(\text{cm}^{-1})$	3598.86	3594.73	3788.34	3646.84
$\nu_2(\text{cm}^{-1})$	1581.71	1589.51	1659.37	1637.77
$\nu_3(\text{cm}^{-1})$	3760.47	3746.07	3895.00	3742.16
$E_{ZPE}^{H_2O}(\text{meV})$	554.242	553.577	579.141	559.557
$E_{molecule}^{H_2O}(\text{eV})$	-490.1756	-490.1768	-490.5789	-490.2454

Table 4. The calculated cohesive energies of icelth per molecule, without and with ZPE (in unit of meV)

	Delocalized - DZP	Localized - DZP	Optimized-DZP	
			Medium	Long
Without ZPE	923.379	897.779	712.311	864.862
With ZPE	782.314	742.993	581.570	731.679

D. Cohesive energy of iceIh

From the calculated vibrational frequencies, it is straightforward to calculate the cohesive energy of ice. The cohesive energy of ice per molecule is expressed as follows:

$$E_{cohesive}^{ice} = (E_{molecule}^{H_2O} + E_{ZPE}^{H_2O}) - (E_{Lattice}^{Ice} + E_{ZPE}^{Ice}) \quad (9)$$

Here the $E_{ZPE}^{H_2O}$ and E_{ZPE}^{Ice} are the correction of the ZPE in an individual water molecule and ice respectively. We have presented the values of the cohesive energy with and without the correction of the ZPE calculated in the various basis sets on Table 4. Our calculated values slightly overestimated the experimental values. The cohesive energy per molecule in ice Ih decreased by around 18.35% in the best numerical atomic basis sets.

Whalley estimated the magnitude of the ZPE, using the known frequencies the vibrational modes of lattice and the individual water molecule, and hence deduced the lattice energy $\Delta E_{Lattice}^{Ice}$ required to convert a non - vibrating crystal at 0K to non - vibrating molecules at the same temperature[17]. The lattice energy $\Delta E_{Lattice}^{Ice}$ arises from the hydrogen bonding and includes contributions from the van der Waals interaction and the closed shell repulsion. As there are two bonds per molecule, it is equivalent to 305.5meV per bond[8]. The energy of a single hydrogen bond in the (H₂O)₂ dimer is 240meV and the observed O-O distance is $2.976 \overset{0}{\text{Å}}$, compared with an inter - site distance of $2.750 \overset{0}{\text{Å}}$ in ice Ih at 0K. The binding in ice is therefore stronger than that in the dimer[8]. Our calculated values of the cohesive energy, calculated by the optimized-DZP basis set with the medium localization, are shown to be near the above value by Whalley, and the binding energy of ice Ih was 4.8% less than the experimental value.

E. The IR spectrum

In the harmonic approximation, we have computed the IR intensities on the each modes for the whole spectra of phonon vibration using the Born effective charge tensor and eigenvectors of normal modes. The transparency of ice to visible

light extends into the near IR range ((14.5–3333)cm⁻¹ or (690–3000)nm), but absorption rises for wavelengths greater than about 1.3μm(8000cm⁻¹) and is very strong over most of the range of (0.0–4000)cm⁻¹. The IR absorption data for H₂O ice in the frequency range of (30 - 4000)cm⁻¹ at 100K is given by Bertie *et al.*[18]. For measurements at the peak around 3225.8cm⁻¹ the sample could only be a few μm thick, but by about 322.6cm⁻¹ several mm were required as the ice passes into the range of low absorption characteristic of microwaves and radio waves. In passing through the frequency range of IR absorption bands, the permittivity falls from the value of 3.16 obtained in the high – frequency limit of electrical measurements to 1.70. This change in permittivity represents the contribution to the electrical polarizability of ice that arises from small displacements of atoms from their equilibrium sites in an electric field[8]. We have also measured the IR absorbance in the vibrational frequency range of (400 - 4000)cm⁻¹ using the IR Prestige 21 spectrometer at the CLNS in the MAS. The results of theoretical and experimental IR absorption for iceIh are presented on Fig.4. The four distinct bands corresponding to the following collective motions: the intra-molecular symmetry and anti-symmetry stretching (ν₁+ ν₃), the bending (ν₂), and the inter-molecular libration (ν_R) and translation (ν_T) are observed.

The intra-molecular motions (the stretching (ν₁+ ν₃) and bending (ν₂)) are called the molecular modes, and these molecular modes are determined by the properties of an individual water H₂O molecule, but modified by interactions with its neighbours, most particularly by the change in the potential well for the protons as a result of hydrogen bonding. In our result, the molecular modes agree with the experimental measurements. The experiment does not distinguish the symmetry and anti-symmetry stretching modes. But the calculation could separate these modes.

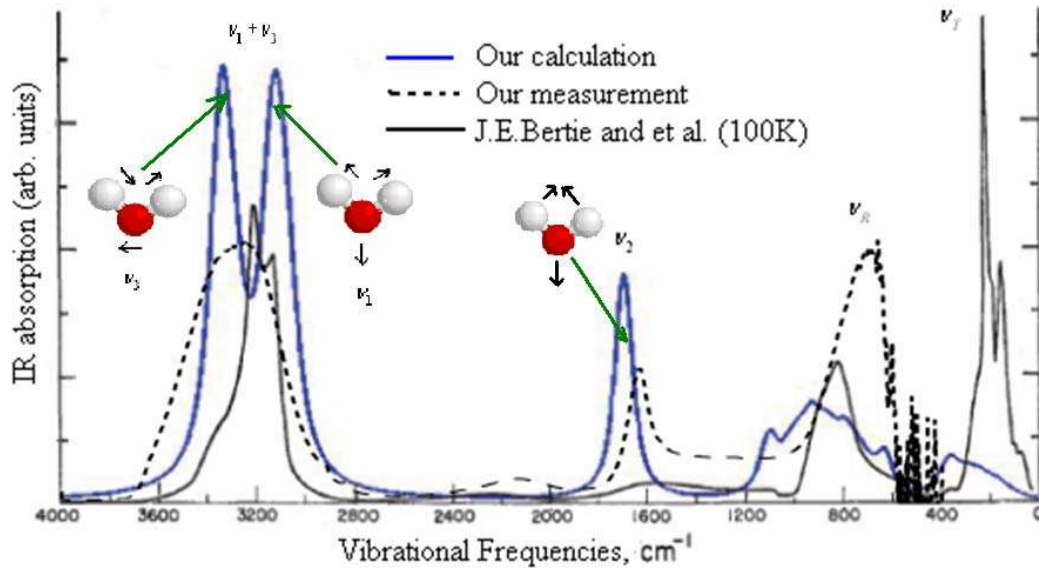


Fig.4. The results of the calculated and measured IR spectra for icelh[14]

The librational modes (motions) are determined by the force acting on a rigid molecule when it is rotated away from its equilibrium position in the lattice. In this case the restoring forces acting are the same as those coupling the motion of one molecule to its neighbours, and this leads to a broad band of frequencies. The coupling between the molecules is relatively weak compared to the forces acting within the molecule. The frequencies of the molecular and librational modes depend on the mass of the hydrogen and deuterium nuclei.

The frequencies of the inter-molecular translational modes (motions) depend on the mass of the whole molecule. Our measurement was not possible to measure in the range of vibrational frequency less than about 400cm^{-1} due to the range of detector in the IR Prestige 21 spectrometer. The IR absorption spectrum does not give us good information regarding the translation motions. But the inelastic incoherent neutron scattering (IINS) measurements give us the more information[19,20]. Using the IINS measurement Li and Ross showed that “*there are two kinds of hydrogen bond*”, depending on the four possible relative orientations of a pair of adjacent molecules in the structure [20].

V. CONCLUSIONS

We have predicted the equilibrium geometry and cohesive energy of the structures of icelh using various basis sets including the ZPE within the supercell approach with periodic boundary conditions. A quantitative description of atomistic structure and dynamics is obtained – an indication of the predictive nature of the approximations used is the (2-3)% overestimated of the typical length of a hydrogen bond. We have computed the IR intensities of icelh on the each mode for the whole spectra of phonon vibration, and measured the IR absorption spectrum in the vibrational frequency range of $(400-4000)\text{cm}^{-1}$. These results were agree with the each other.

Acknowledgement

This work was supported by Mongolian Government’s Innovation Development Program under the project No. H.1.5.1. and the Mongolian Foundation for Science and Technology. We thank to Dr. A. Chemidtsogzol, who measured the IR absorption spectrum of ice.

References:

1. D.Porezag and M.R.Pederson, *Phys. Rev. B.*, **54**, 7830 (1996).
2. D.Fernandez-Torre and *et al.*, *J.Phys.Chem.A.*, **108**, 10535 (2004)

3. R.D.King-Smith and D.Vanderbilt, *Phys. Rev.B.*, **47**, 1651 (1993)
4. M.Bernasconi and *etc.*, *Phys. Rev. Lett.*, **81**, 1235 (1998)
5. J.M.Soler and *et.al.*, *J.Phys.:Condens.Matter*, **14**, 2745 (2002)
6. E.Artacho and *et al.*, *J.Phys.:Condens.Matter*, **20**, 064208 (2008)
7. J.D.Bernal and R.H.Fowler, *J.Chem.Phys.*, **1**, 515 (1933)
8. V.F.Petrenko and R.W.Whitworth, *Physics of Ice*, Oxford University Press, (2002)
9. K.Rottger and *et al.*, *Acta Crystallographica*, **B50**, 644 (1994)
10. C.M.B.Line and R.W.Whitworth, *J.Chem.Phys.*, **104**, 10008 (1996)
11. I.Morrison and *et al.*, *J.Phys.Chem.B.*, **101**, 6147 (1997)
12. H.J.Monkhorst and J.D.Pack, *Phys. Rev.B.*, **13**, 5188 (1976)
13. N.Tsogbadrakh, *Ph.D. Thesis*, University of Salford, Salford, England, (2006)
14. Sh.Dashpurev, *MSc. Thesis*, National University of Mongolia, Ulaanbaatar, Mongolia, (2010)
15. H.P.Hobbs, *Ice Physics*, Oxford University Press, (1974)
16. W.S.Benedict and *et al.*, *J.Chem.Phys.*, **24**, 1139 (1956)
17. E.Whalley, *Transactions of the Faraday Society*, **53**, 1578 (1957)
18. J.E.Bertie and *et al.*, *J.Chem.Phys.*, **50**, 4501 (1969)
19. J.-C.Li and D.K.Ross, In *Physics and chemistry of ice* (edited by N.Maeno and T.Hondoh), Hokkaido University Press, Sapporo, 27(1992)
20. J.-C.Li and D.K.Ross, *Nature*, **365**, 327 (1993)